

Finite element modeling of the vibrational behavior of multi-walled nested silicon-carbide and carbon nanotubes

Abed Nikkar¹, Saeed Rouhi^{*2} and Reza Ansari¹

¹Department of Mechanical Engineering, University of Guilan, P.O. Box 3756, Rasht, Iran

²Young Researchers and Elite Club, Langarud Branch, Islamic Azad University, Langarud, Guilan, Iran

(Received May 30, 2016, Revised July 8, 2017, Accepted July 19, 2017)

Abstract. This study concerns the vibrational behavior of multi-walled nested silicon-carbide and carbon nanotubes using the finite element method. The beam elements are used to model the carbon-carbon and silicon-carbon bonds. Besides, spring elements are employed to simulate the van der Waals interactions between walls. The effects of nanotube arrangement, number of walls, geometrical parameters and boundary conditions on the frequencies of nested silicon-carbide and carbon nanotubes are investigated. It is shown that the double-walled nanotubes have larger frequencies than triple-walled nanotubes. Besides, replacing silicon carbide layers with carbon layers leads to increasing the frequencies of nested silicon-carbide and carbon nanotubes. Comparing the first ten mode shapes of nested nanotubes, it is observed that the mode shapes of armchair and zigzag nanotubes are almost the same.

Keywords: dynamic analysis; finite element method; numerical methods; size effect; nanostructures/nanotubes

1. Introduction

High mechanical strength, high thermal conductivity, and variable band gap of silicon carbide (SiC) (Hanchen and Ghoniem 1993, Morkoc *et al.* 1994, Persson and Lindefelt 1996), similar to those of carbon nanotubes (CNTs) (Hajnayeb and Khadem 2015, Ebrahimi *et al.* 2016), make it as a great candidate to be utilized in severe environment such as high temperature, high power, and high frequency. These unique properties of bulk SiC have attracted the attention of the research community to investigate the properties of SiC nanostructures. For example, different groups have synthesized SiC nanotubes, successfully (Nhut *et al.* 2002, Sun *et al.* 2002, Borowiak-Palen *et al.* 2005, Huczko *et al.* 2005, Pei *et al.* 2006).

Mechanical behavior of SiC nanostructures has been investigated by different researchers. The behavior of SiC nanotubes under tensile strain was explored by Pan and Si (2009) by using molecular dynamics (MD) simulations. They showed that the mechanical properties of SiC nanotubes are approximately independent of the nanotube diameter. The values of 465 Gpa and 540 Gpa were obtained for Young's modulus of SiC nanotubes with the wall thicknesses of 0.3 nm and 0.9 nm, respectively.

Employing MD simulations, tensile and compressive behaviors of twinned silicon carbide nanowires (SiCNWs) were investigated by Wang *et al.* (2010). It was shown that twin stacking fault lead to enhancing the critical strain of the twinned nanowires. Lin *et al.* (2010) obtained the bulk modulus of SiCNWs as 316 Gpa. First-principles calculations were used by Zhang *et al.* (2012) to study the

elastic properties of single-walled SiC nanotubes. They showed that Young's modulus of single-walled SiC nanotubes directly depends on the nanotube diameter. The in situ tensile tests were employed by Cheng *et al.* (2014) to evaluate the mechanical characterization of SiC nanowires. It was observed that SiC nanowires experience elastically linear deformation until the brittle fracture.

Le (2014a) used molecular mechanics to predict Young's modulus of graphene, boron nitride (BN), SiC nanosheets and their nanotubes. The elastic moduli of SiC nanosheets were obtained as 149.7 Gpa and 149.5 Gpa for zigzag and armchair nano sheets, respectively. Besides, Young's modulus of SiC nanotubes were computed in the range of 120 – 148 N/m.

The mechanical behavior of hexagonal aluminum nitride (AlN), BN, gallium nitride (GaN), indium nitride (InN), and SiC monolayer sheets under tensile loading was studied by Le by using MD simulations (Le 2014b). It was shown that Young's modulus of BN, SiC, AlN, InN, and GaN nanosheets are approximately 77%, 53%, 41%, 27% and 25% Young's modulus of graphene, respectively.

Setoodeh and Atriani (2009) used MD simulations to investigate the buckling behavior of SiC nanotubes. They showed that Young's modulus of SiC nanotubes does not depend on the nanotube chirality and diameter. Depending on the nanotube length, two types of buckling were observed, including local and global buckling. The buckling behavior of SiC nanotubes were also studied by Ansari *et al.* (2012) by using a 3D finite element (FE) approach. They showed that the critical buckling force of single-walled SiC nanotubes decreases by increasing nanotube aspect ratio. They also showed that the critical buckling force of single-layered SiC nanosheets is size dependent (Ansari *et al.* 2013). Ansari *et al.* (2015) studied the axial buckling behavior of multi-walled SiC nanotubes by using

*Corresponding author, Ph.D.
E-mail: s_rouhi@iaul.ac.ir

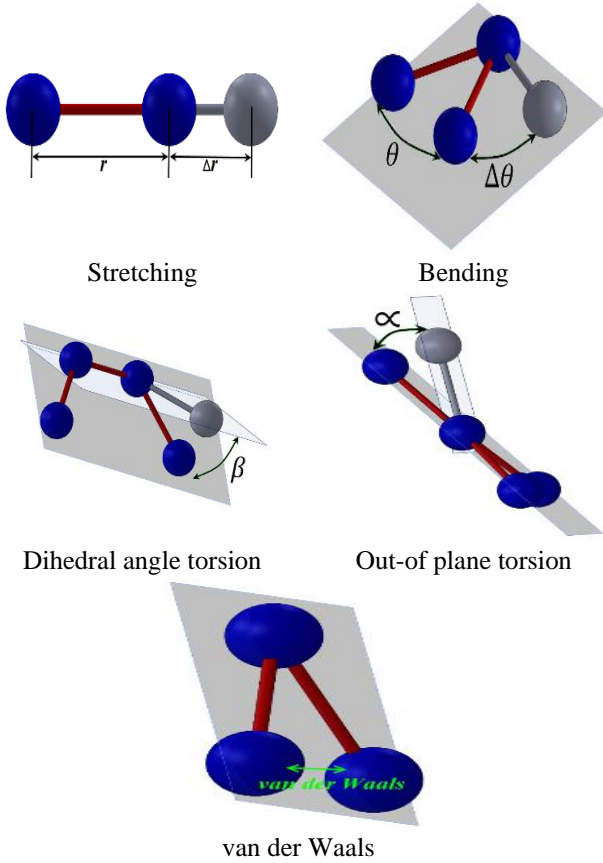


Fig. 1 Schematic of energy terms in molecular mechanics

a molecular mechanics model. They showed that the nanotubes with more walls are less stable than those with less walls.

The vibrational characteristics of single-walled SiC nanotubes were studied by Khani *et al.* (2014) by using FE method. They showed that the nanotubes with smaller lengths have larger frequencies than those with larger lengths. Ansari and Rouhi (2016) studied the vibrational behavior of silicon carbide nanosheets and SiC nanotubes. They showed that increasing the size of nanosheet leads to decreasing their frequencies. Besides, the effect of nanotube boundary conditions on the nanotube frequencies is more prominent for smaller single-walled SiC nanotubes.

The FE approach is used here to study the vibrational behavior of nested carbon nanotubes and SiC nanotubes. To this end, double-walled and triple-walled nanotubes are considered. The effects of nanotube length and boundary conditions on the vibrational behavior of nested CNTs and SiC nanotubes are studied. The frequencies and mode shapes of nanotubes are extracted.

2. Molecular structural model

Considering the equivalency of the molecular mechanics and structural mechanics, a FE approach has been developed which can be used to study the mechanical behavior of nanostructures (Odegard *et al.* 2002, Li and Chou 2004). To this end, the total energy of a molecular

Table 1 The force constants and bond lengths

	C-C (Leach 1996)	Si-C (Ansari <i>et al.</i> 2012, Ansari <i>et al.</i> 2013)
k_r	$6.52 \times 10^{-7} \text{ N/nm}$	$4.17 \times 10^{-7} \text{ N/nm}$
k_θ	$8.76 \times 10^{-10} \text{ Nnm/rad}^2$	$8.42 \times 10^{-10} \text{ Nnm/rad}^2$
k_τ	$2.78 \times 10^{-10} \text{ Nnm/rad}^2$	$1.505 \times 10^{-9} \text{ Nnm/rad}^2$
L	1.421 Å	1.786 Å

system is expressed as the summation of the energies shown in Fig. 1 as

$$U_{total} = \sum U_r + \sum U_\theta + \sum U_\phi + \sum U_\omega + \sum U_{vdw} \quad (1)$$

in which U_r , U_θ , U_ϕ and U_ω are the bonding energies which are related to bond stretching, bond angle bending, dihedral angle torsion, out-of plane torsion energies, respectively. Besides, U_{vdw} is the nonbonding vdW energy. The last term can be neglected compared to other terms in the single-walled structures. Besides, the two torsion terms are compacted in one term. Considering k_r , k_θ and k_τ as force constant of the stretching, force constant of the bending and force constant of the torsion, respectively and Δr , $\Delta\theta$ and $\Delta\phi$ as bond length variation, bond angle variation and angle variation from equilibrium position, respectively, the remaining energy terms are expressed as (Gelin 1994, Leach 1996)

$$U_r = \frac{1}{2} k_r (r - r_0)^2 = \frac{1}{2} k_r (\Delta r)^2 \quad (2)$$

$$U_\theta = \frac{1}{2} k_\theta (\theta - \theta_0)^2 = \frac{1}{2} k_\theta (\Delta\theta)^2 \quad (3)$$

$$U_\tau = U_\phi + U_\omega = \frac{1}{2} k_\tau (\Delta\phi)^2 \quad (4)$$

Table 1 shows the Si-C, and C-C force constants. As it was previously mentioned, the van der Waals interaction is ignored here. This is because the smaller portion of the van der Waals interaction energy compared to the other energies. The van der Waals energy is expressed as

$$U(R) = 4\varepsilon \left[\left(\frac{\sigma}{R} \right)^{12} - \left(\frac{\sigma}{R} \right)^6 \right] \quad (5)$$

where ε and σ are the Lennard–Jones parameters and R is the distance between atoms. Considering the values of $\varepsilon = 5.4071 \times 10^{-12} \text{ NÅ}$ and $\sigma = 3.4 \text{ Å}$, the van der Waals interaction energy is equal to $5.13 \times 10^{-11} \text{ NÅ}$ for the two carbon atoms located at the distance of 3 Å from each other. While, by only 1 Å increase of the bond length one can obtain the U_r as $6.52 \times 10^{-8} \text{ NÅ}$, which is 1271 times the van der Waals interaction. Therefore, van der Waals energy is neglected.

To obtain the element properties, the corresponding energies of a beam element in the structural mechanics should be considered which are stated as

$$U_A = \frac{1}{2} \int_0^L \frac{N^2}{EA} dL = \frac{1}{2} \frac{N^2 L}{EA} = \frac{1}{2} \frac{EA}{L} (\Delta L)^2 \quad (6)$$

Table 2 C-C and Si-C element properties

	C-C	Si-C
$E \left(\frac{N}{\text{Å}^2} \right)$	5.488×10^{-8}	2.9372×10^{-8}
$G \left(\frac{N}{\text{Å}^2} \right)$	8.701×10^{-9}	2.6256×10^{-8}
$d(\text{Å})$	1.466	1.7971

$$U_M = \frac{1}{2} \int_0^L \frac{M^2}{EI} dL = \frac{2EI}{L} \alpha^2 = \frac{1}{2} \frac{EI}{L} (2\alpha)^2 \quad (7)$$

$$U_T = \frac{1}{2} \int_0^L \frac{T^2}{GJ} dL = \frac{1}{2} \frac{T^2 L}{GJ} = \frac{1}{2} \frac{GJ}{L} (\Delta\beta)^2 \quad (8)$$

In the above equation, N , M and T are tensional force, bending moment and torsional moment applied to the beam elements and ΔL , α and $\Delta\beta$ are length variation due to N , bending angle due to M and torsion angle due to T , respectively. E , L , A , I , J and G are Young's modulus, length, cross-sectional area, moment of inertia, polar moment of inertia and shear modulus of beam elements which should be computed. By equating the corresponding energy terms in molecular and structural mechanics, one would have

$$\begin{aligned} \frac{EA}{L} &= k_r \\ \frac{EI}{L} &= k_\theta \\ \frac{GJ}{L} &= k_\tau \end{aligned} \quad (9)$$

Considering the circular cross section for the beam elements, their properties are obtained as functions of force constants (Ansari and Rouhi 2010, Rouhi and Ansari 2012)

$$d = 4 \sqrt{\frac{k_\theta}{k_r}}, E = \frac{k_r^2 L}{4\pi k_\theta}, G = \frac{k_r^2 k_\tau L}{8\pi k_\theta^2} \quad (10)$$

Substituting the values given in Table 1 into the above equations, the properties of beams representing the Si-C and C-C bonds are obtained as Table 2. 6-12 Lennard-Jones potential function is used to simulate the vdW interactions between different walls

$$U(R) = 4\epsilon \left[\left(\frac{\sigma}{R} \right)^{12} - \left(\frac{\sigma}{R} \right)^6 \right] \quad (11)$$

where R is the distance between atoms and ϵ and σ are Lennard-Jones parameters. Here, spring elements are used to model the van der Waals interactions whose stiffness are obtained by differentiating Eq. (11) as

$$k_{vdw} = 24\epsilon \left(26 \frac{\sigma^{12}}{R^{14}} - 7 \frac{\sigma^6}{R^8} \right) \quad (12)$$

The ϵ and σ constants for Si-C, and C-C pairs are given in Table 3. Substituting these values in Eq. (11), the Si-C and C-C spring constants are obtained as functions of inter-atomic distances. The cut-off distance for spring elements is considered as 2.5σ . Finally, the mass elements of $1.9943 \times$

Table 3 ϵ and σ constants for Si-C, C-C and Si-Si pairs

	ϵ	σ
Si-C	$1.5186 \times 10^{-11} \text{NÅ}$	3.1 Å
C-C	$5.4071 \times 10^{-12} \text{NÅ}$	3.4 Å
Si-Si	$4.2632 \times 10^{-11} \text{NÅ}$	2.8 Å

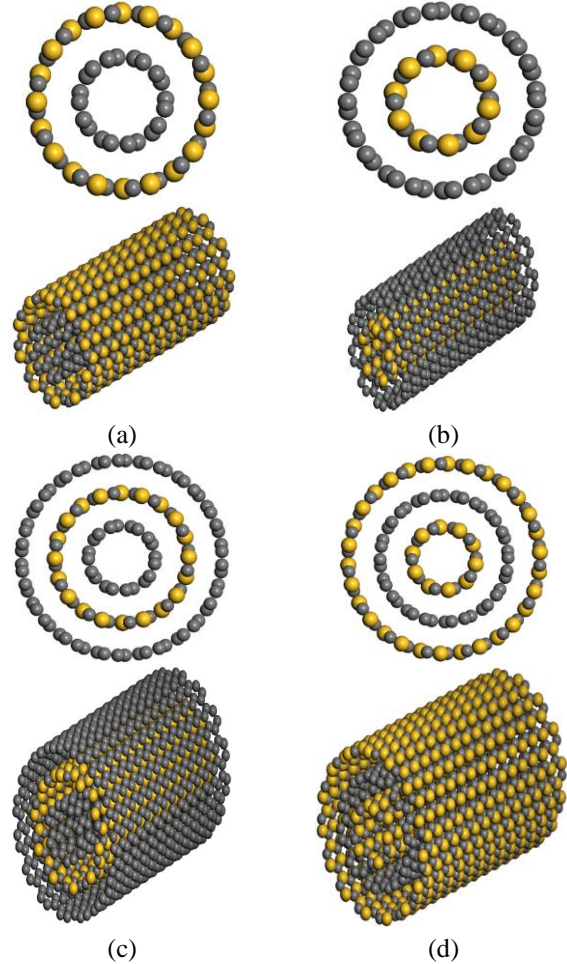


Fig. 2 Concentric (a) C-SiC DWNT, (b) SiC-C DWNT, (c) C-SiC-C TWNT and (d) SiC-C-SiC TWNT

10^{-26}kg and $4.6646 \times 10^{-26} \text{kg}$ are used instead of C and Si atoms, respectively.

3. Results and discussion

In this section, the frequencies of concentric SiC nanotubes and CNTs (Fig. 2) are obtained using the described FE model. To compute the natural frequencies, the approach described by Ansari *et al.* (2016), Rouhi *et al.* (2016), Shahnazari *et al.* (2017) is used. The first and second material in the name of double-walled nested SiC nanotube and CNT nanotubes show the inner and outer walls. Similarly, in triple-walled nested SiC nanotube and CNT nanotubes, the first, second and third numbers show the inner, middle and outer layers. As it was mentioned, the covalent bonds and noncovalent van der Waals interactions are modeled by beam and spring elements, respectively (see

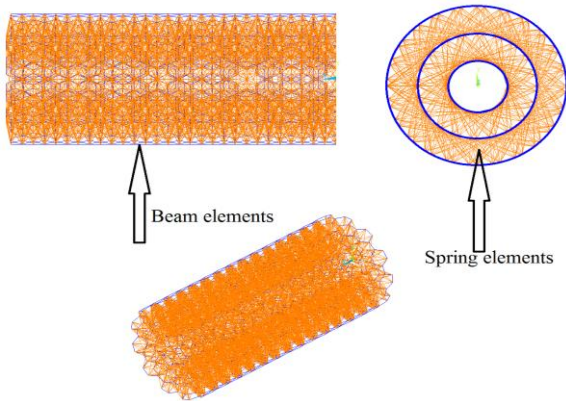


Fig. 3 Schematic of beam and spring elements

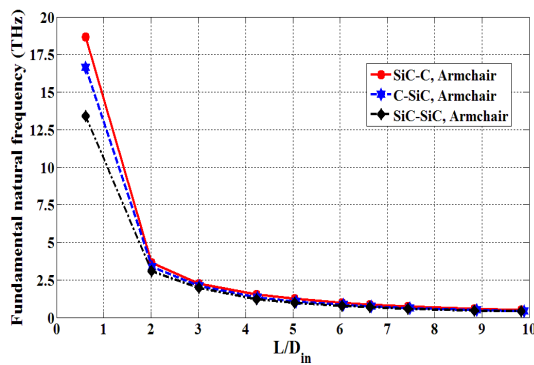


Fig. 4 First natural frequencies of concentric SiC-SiC, Si-C and C-Si armchair nanotubes with the inner radius of 3.41 \AA under clamped-clamped boundary conditions versus nanotube aspect ratio

Fig. 3). The influences of nanotube aspect ratio (length/inner radius), the order of arrangements and boundary conditions on the vibrational behavior of concentric SiC and C nanotubes are studied.

3.1 Double-walled concentric SiC nanotubes and CNTs

In Fig. 4 the fundamental natural frequencies of concentric SiC and C nanotubes are compared with those of double-walled SiC nanotubes. Increasing the nanotube aspect ratio leads to decreasing the frequencies of double walled nanotubes (DWNTs). The rate of reduction is larger at initial parts of the curves. It can be seen that the substituting a Si tube in the double-walled SiC nanotubes by a CNT leads to increasing the natural frequencies of the DWNTs. However, increasing aspect ratio results in decreasing the difference between the curves. For example, at the aspect ratio of 1, the natural frequencies of the SiC-C, C-SiC and SiC-SiC nanotubes are equal to 18.65 THz, 16.62 THz, 13.41 THz, respectively. Besides, the associated values are equal to 2.26 THz, 2.08 THz and 1.97 THz, respectively, at the aspect ratio of 3.

Fig. 5 shows the fundamental natural frequencies of the SiC-C and C-SiC DWNTs under clamped-clamped boundary conditions. Here, the armchair and zigzag nanotubes are considered with the inner radii of 3.41 \AA and

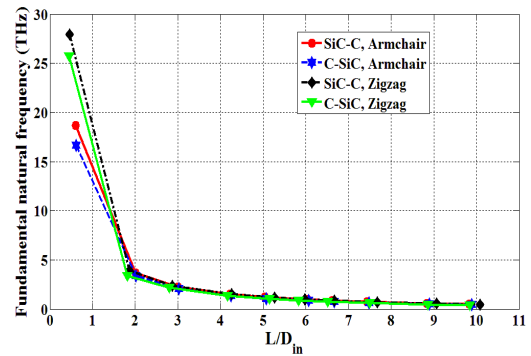


Fig. 5 Fundamental natural frequencies of concentric SiC-C and C-SiC armchair and zigzag DWNTs with the inner radii of 3.41 \AA and 3.45 \AA under clamped-clamped boundary conditions versus nanotube aspect ratio

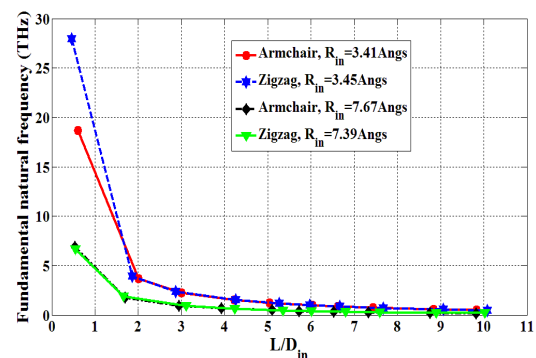


Fig. 6 Fundamental natural frequencies of concentric SiC-C DWNTs with different inner radii under clamped-clamped boundary conditions versus nanotube aspect ratio

3.45 \AA , respectively. It is seen that the SiC-C nanotubes possess larger frequencies than C-SiC nanotubes. This can be related to the larger stiffness of C-C bonds than Si-C bonds (see Table 2) and smaller masses of C atoms than Si atoms. As the outer layer of the DWNTs has more bonds and atoms, according to the frequency equation ($\sqrt{k/m}$), larger stiffness and smaller mass leads to larger frequencies. However, the difference is only observable for the initial region of the curves. So, it can be concluded that the effect of nanotube layer order on the vibrational behavior of concentric SiC and C DWNTs is only significant for small aspect ratios.

It is also seen that the zigzag nanotubes possess larger frequencies than armchair ones. This has been previously observed for DWCNTs (Ansari *et al.* 2016). However, after the aspect ratio of 2, the difference between the natural frequencies of armchair and zigzag nanotubes disappears for both of the SiC-C and C-SiC DWNTs.

Fig. 6 depicts the influence of the nanotube inner radius on the fundamental natural frequencies of clamped-clamped armchair and zigzag concentric SiC-C DWNTs. It is observed that the nanotubes with larger radii would have smaller frequencies. For example, at the aspect ratio of 1, the fundamental natural frequencies of the clamped-clamped armchair nanotubes with the inner radii of 3.41 \AA and 7.67 \AA are about 18.65 THz and 6.89 THz,

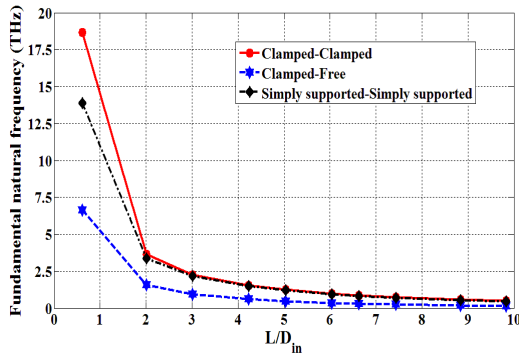


Fig. 7 Effect of boundary conditions on the fundamental natural frequencies of concentric armchair SiC-C DWNTs with the inner radius of 3.41 Å

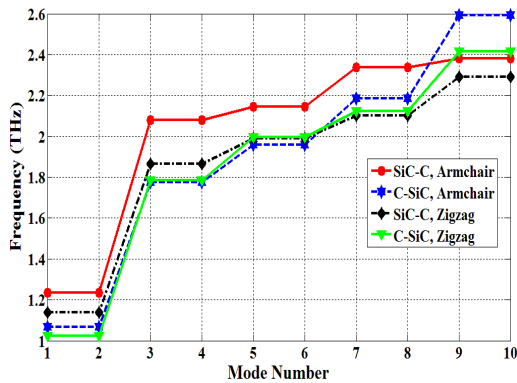


Fig. 8 First ten natural frequencies of concentric SiC-C and C-SiC armchair and zigzag DWNTs with the inner radii of 3.41 Å and 3.45 Å and aspect ratio of 5 under clamped-clamped boundary conditions

respectively, which shows 170.68% difference. Besides, the frequencies of the zigzag nanotubes with the radii of 3.45 Å and 7.39 Å are equal to 27.95 THz and 6.69 THz, which represents 317.78% difference. So, one can conclude that the increased mass by increasing the radius of nanotubes is more than increasing the stiffness. The difference between the frequencies of armchair and zigzag DWNTs is more prominent at smaller radii. Increasing the aspect ratio leads to decreasing the effect of geometry on the frequencies of armchair and zigzag nanotubes. For example, at the aspect ratio of 4, the frequencies of the armchair nanotubes with the inner radii of 3.41 Å and 7.67 Å are equal to 1.53 THz and 0.67 THz, respectively. The corresponding values of the zigzag nanotubes with the aspect ratio of 4 are 1.51 THz and 0.64 THz, respectively. Therefore, the difference percentages are about 128.36% and 135.94% for the armchair and zigzag nanotubes, respectively, which are smaller than the associated difference percentages at the aspect ratio of 1. Fig. 7 shows the frequencies of an armchair SiC-C nanotube with the inner radius of 3.41 Å versus the nanotube aspect ratio. It can be seen the largest and smallest frequencies associate with the clamped-clamped and clamped-free nanotubes, respectively. Besides, after the aspect ratio of 3, the curve associated with clamped-clamped and simply supported-simply supported nanotubes coincide. For example, at the aspect

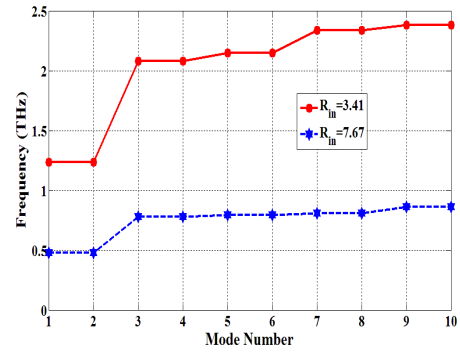


Fig. 9 First ten natural frequencies of concentric armchair SiC-C DWNTs with the aspect ratio of 5 under clamped-clamped boundary conditions

ratio of 1, the frequencies of the clamped-clamped, clamped-free and simply supported-simply supported nanotubes are equal to 18.65 THz, 6.64 THz and 13.89 THz, respectively. Besides, for the aspect ratio of 5, the corresponding frequencies are obtained as 1.24 THz, 0.47 THz and 1.21 THz, respectively. Therefore, it can be concluded that the effect of constraining rotational degrees of freedom is only important for small aspect ratios.

The first ten natural frequencies of armchair and zigzag concentric SiC-C and C-SiC DWNTs are given in Fig. 8. The inner radii of armchair and zigzag DWNTs are selected as 3.41 Å and 3.45 Å, respectively. Besides, the aspect ratio is selected as 5. It is observed that for all of the nanotubes, a sudden mutation happens at the third frequencies and after that the frequencies increase with lower intensity. Besides, the effect of inner radius of the nanotubes on the first natural frequencies is shown in Fig. 9. It is observed that the distance between the curves is at larger modes.

The first ten mode shapes of nested armchair and zigzag SiC-C DWNTs are given in Figs. 10 and 11. The inner radii of nanotubes are selected as 3.41 Å and 3.45 Å, respectively. Besides, the aspect ratio is considered as 7. It can be seen that the corresponding mode shapes of armchair and zigzag nanotubes are almost the same. Besides, a sudden change between the second and third modes is observed that verifies the sudden increase between the second and third frequencies of the nanotubes.

3.2 Triple-walled concentric SiC nanotubes and CNTs

The effect of substituting a SiC layer in the structure triple-walled nanotubes (TWNTs) by one or two C layers was studied in Fig. 12. It can be seen that the larger number of C layers in the TWNTs leads to larger frequencies. This result could be predicted based on the larger stiffness of C-C than Si-C bonds and smaller atomic masses of C than Si atoms. The fundamental natural frequencies of concentric SiC and C TWNTs are plotted in Fig. 13 against the nanotube aspect ratio. It can be observed that as DWNTs, zigzag TWNT have larger frequencies than armchair ones. Besides, as it can be predicted, the TWNTs with two CNT layers have larger frequencies than those with two SiC nanotube layers. The effect of chirality and order of layers

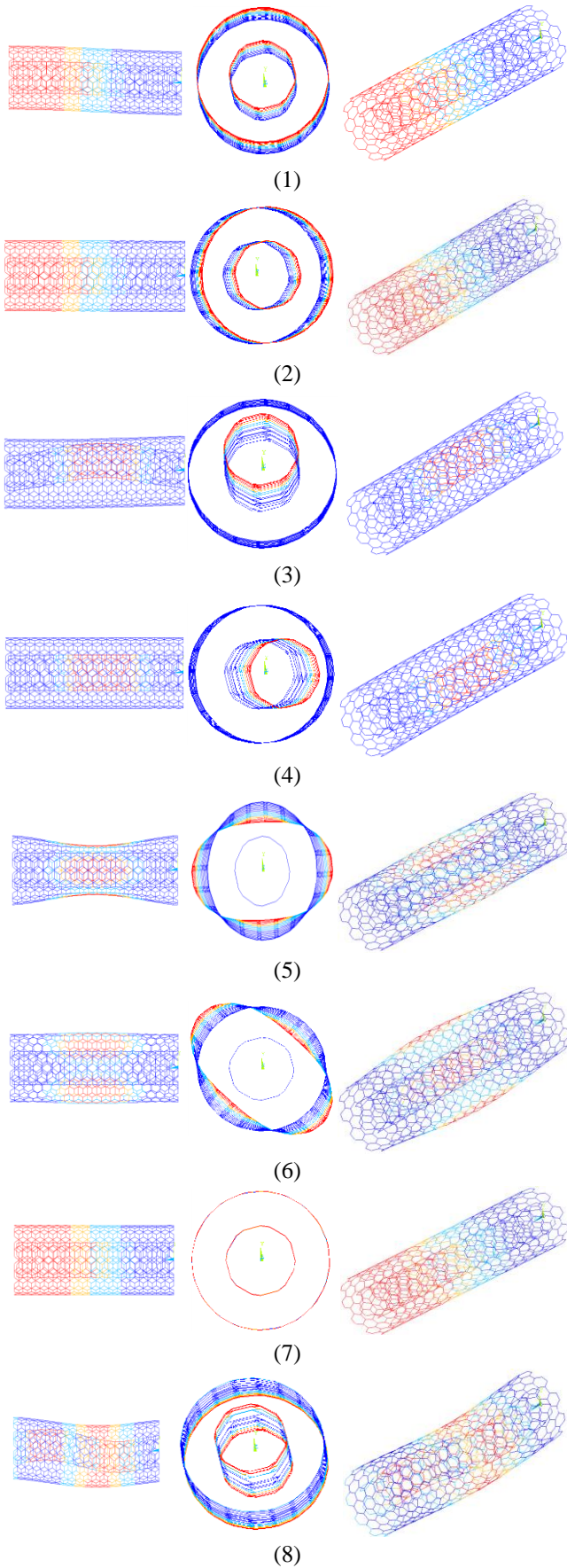


Fig. 10 First ten mode shapes of concentric armchair SiC-C DWNT with the inner radius of 3.41 Å and aspect ratio of 7 under clamped-free boundary conditions

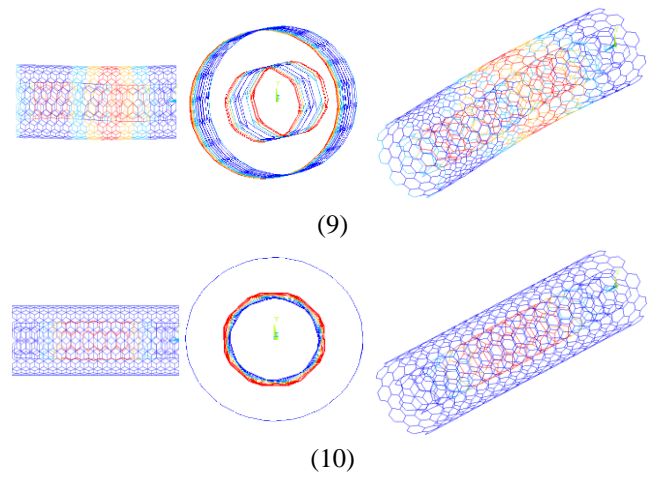


Fig. 10 Continued

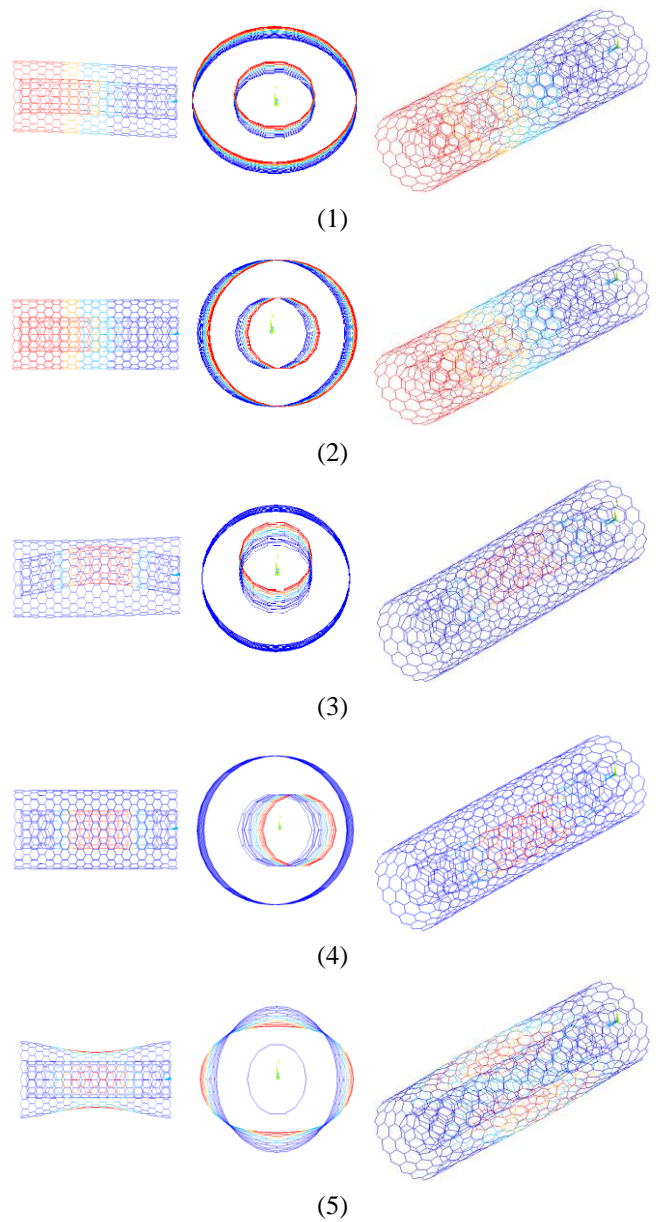


Fig. 11 First ten mode shapes of concentric zigzag SiC-C DWNT with the inner radius of 3.45 Å and aspect ratio of 7 under clamped-free boundary conditions

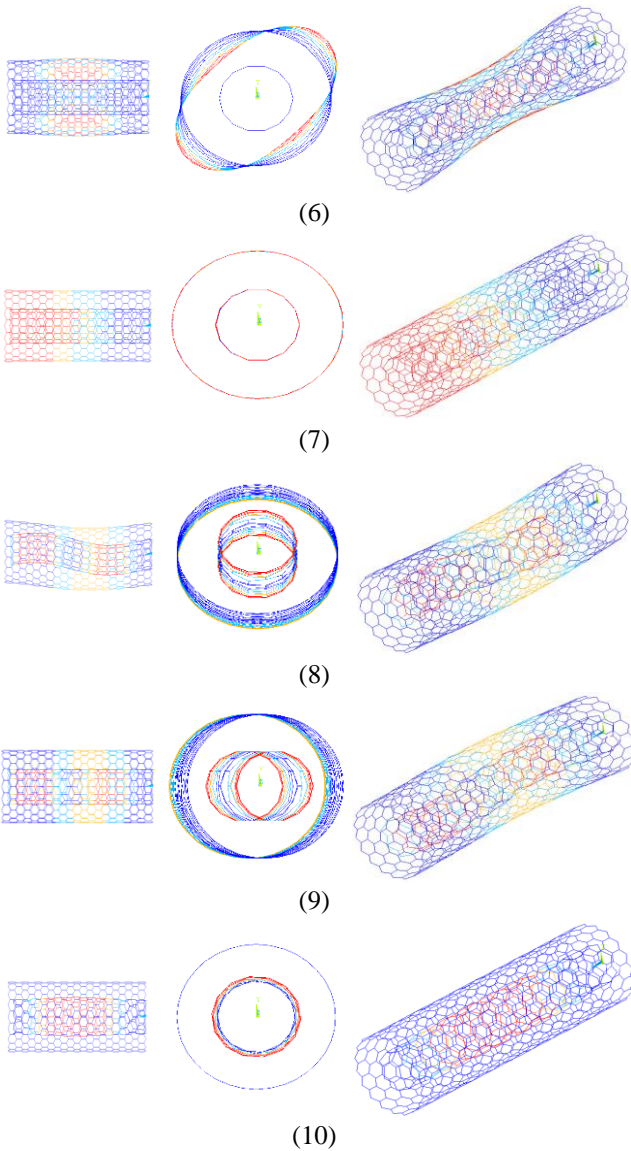


Fig. 11 Continued

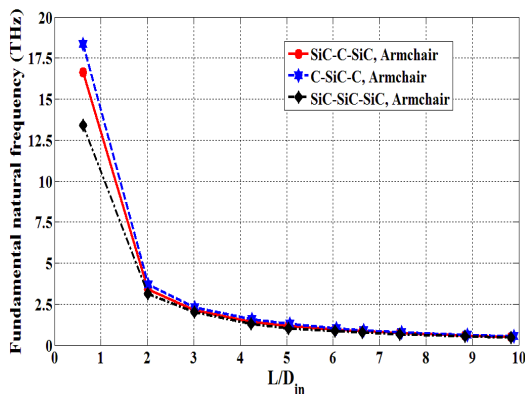


Fig. 12 First natural frequencies of concentric armchair SiC-SiC-SiC, Si-C-SiC and C-SiC-C nanotubes with the inner radius of 3.41 Å under clamped-clamped boundary conditions versus nanotube aspect ratio

is more prominent for TWNTs under clamped-clamped boundary conditions.

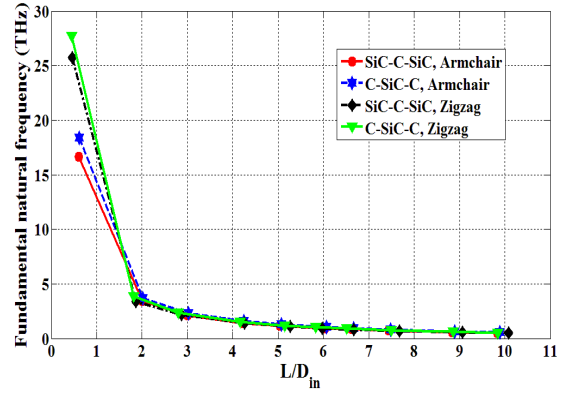


Fig. 13 Fundamental natural frequencies of concentric SiC and C armchair and zigzag TWNTs with the inner radii of 3.41 Å and 3.45 Å under clamped-clamped boundary conditions versus nanotube aspect ratio

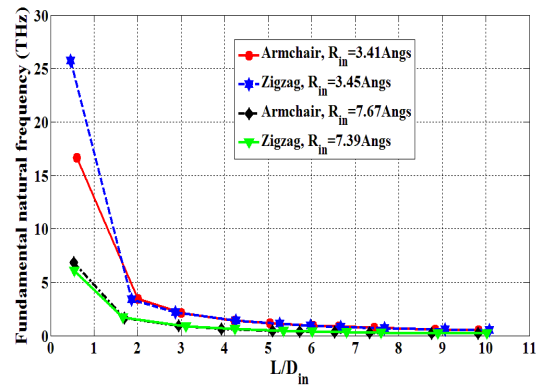


Fig. 14 Fundamental natural frequencies of concentric SiC-C-SiC TWNTs under clamped-clamped boundary conditions versus nanotube aspect ratio

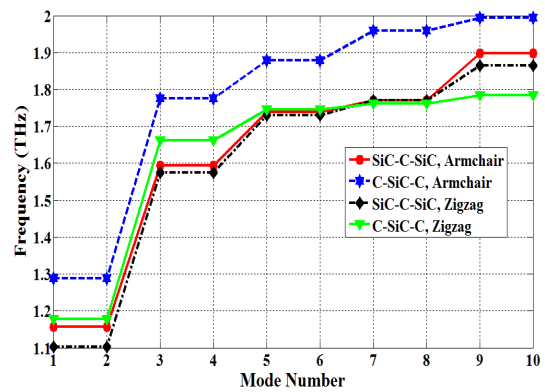


Fig. 15 First ten natural frequencies of concentric SiC-C-SiC and C-SiC-C armchair and zigzag TWNTs with the inner radius of 3.41 Å and 3.45 Å and aspect ratio of 5 under clamped-clamped boundary conditions

The effect of the radius of the concentric SiC and C TWNTs is studied in Fig. 14. It is seen that TWNTs with larger radii possess smaller frequencies. However, the effect of nanotube radii on the frequencies of TWNTs is only significant of the aspect ratios smaller than 2. Moreover, it is clear that increasing the aspect ratio leads to decreasing the difference between the frequencies of the

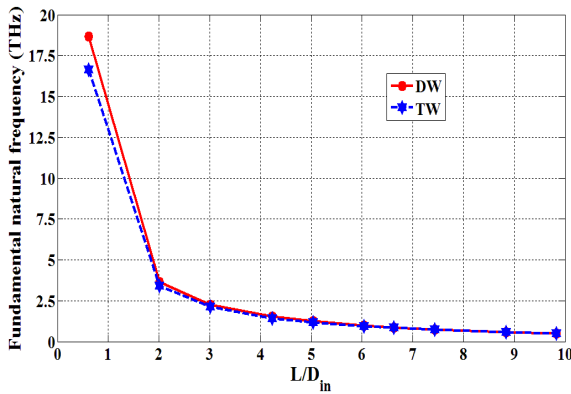


Fig. 16 Comparison of the fundamental natural frequencies of armchair SiC-C DWNT and SiC-C-SiC TWNT with the inner radius of 3.41 Å under clamped-clamped boundary conditions versus aspect ratio

nanotubes. So, it can be concluded that the effect of geometry diminishes for sufficiently long nanotubes.

The first ten natural frequencies of SiC-C-SiC and C-SiC-C armchair and zigzag TWNTs are given in Fig. 15. The inner radius of armchair and zigzag TWNTs are considered as 3.41 Å and 3.45 Å, respectively. Besides, the aspect ratio is selected as 5. Clamped-clamped boundary condition is applied to the ends of the nanotubes. It is observed that all of the curves experience a parallel path with a sudden jump between the second and third frequencies. For all of the curves, after the third frequencies, a slight increase happens between even and odd frequencies.

3.3 Comparison of double-walled and triple-walled concentric SiC nanotubes and CNTs

In this section, the vibrational behavior of concentric SiC and C DWNTs and TWNTs are compared. Represented in Fig. 16 is the Fundamental natural frequencies of SiC-C DWNT and SiC-C-SiC TWNT. The inner radius of nanotubes is selected as 3.41 Å and clamped-clamped boundary conditions are applied to the edges of DWNT and TWNT. It is observed that the fundamental natural frequencies of DWNTs are larger than those of TWNTs. However, two curves converge for long nanotubes. The first ten frequencies of DWNTs and TWNTs with the inner radius of 3.41 Å and aspect ratio of 5 are drawn in Fig. 17. Comparing two curves, it is seen that all of the frequencies of DWNTs are larger than those of TWNTs. The difference is larger for higher modes.

4. Conclusions

In this paper, the vibrational characteristics of multi-walled nested SiC nanotubes and CNTs were investigated. The beam and mass elements were used to model the bonding and nonbonding interactions. Besides, the atoms were substituted by mass elements. It was observed that the effect of Si and C layer order is only significant for small

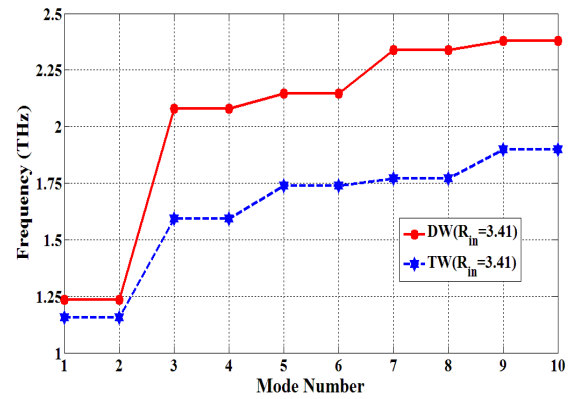


Fig. 17 Comparison of the first ten natural frequencies of armchair SiC-C DWNT and SiC-C-SiC TWNT with the inner radius of 3.41 Å and aspect ratio of 5 under clamped-clamped boundary conditions versus aspect ratio

aspect ratios. Besides, investigating the effect of nanotube inner radii on their frequencies, it was shown that nested nanotubes with smaller radii have larger frequencies. It was also shown that the frequencies of multi-walled nested SiC nanotubes and CNTs decrease by increasing the number of walls. The difference is more significant at higher modes. Nanotubes with clamped-clamped boundary conditions exhibit frequencies larger than those with clamped-free and simply supported ones. However, the difference between clamped-clamped and simply supported nanotubes is more distinguishable for small nanotubes.

References

- Ansari, R. and Rouhi, S. (2010), "Atomistic finite element model for axial buckling of single-walled carbon nanotubes", *Physica E: Low-Dimens. Syst. Nanostruct.*, **43**(1), 58-69.
- Ansari, R., Rouhi, S., Aryayi, M. and Mirnezhad, M. (2012), "On the buckling behavior of single-walled silicon carbide nanotubes", *ScientiaIranica*, **19**(6), 1984-1990.
- Ansari, R., Rouhi, S., Mirnezhad, M. and Aryayi, M. (2013), "Stability characteristics of single-layered silicon carbide nanosheets under uniaxial compression", *Physica E: Low-Dimens. Syst. Nanostruct.*, **53**, 22-28.
- Ansari, R., Mirnezhad, M. and Rouhi, H. (2015), "Buckling of multi-walled silicon carbide nanotubes under axial compression via a molecular mechanics model", *Appl. Phys. A*, **118**(3), 845-854.
- Ansari, R., Rouhi, S. and Aryayi, M. (2016), "On the vibration of double-walled carbon nanotubes using molecular structural and cylindrical shell models", *Int. J. Modern Phys. B*, **30**(5), 1650007.
- Ansari, R. and Rouhi, S. (2016), "Vibrational analysis of single-layered silicon carbide nanosheets and single-walled silicon carbide nanotubes using nanoscale finite element method", *Proc. Inst. Mech. Eng., Part C: J. Mech. Eng. Sci.*, **231**(18), 0954406216645129.
- Borowiak-Palen, E., Ruemmel, M.H., Gemming, T., Knupfer, M., Biedermann, K., Leonhardt, A., Pichler, T. and Kalenczuk, R.J. (2005), "Bulk synthesis of carbon-filled silicon carbide nanotubes with a narrow diameter distribution", *J. Appl. Phys.*, **97**(5), 056102.
- Cheng, G., Chang, T.H., Qin, Q., Huang, H. and Zhu, Y. (2014),

- “Mechanical properties of silicon carbide nanowires: effect of size-dependent defect density”, *Nano Lett.*, **14**(2), 754-758.
- Ebrahimi, F., Shaghghi, G.R. and Boreiry, M. (2016), “An investigation into the influence of thermal loading and surface effects on mechanical characteristics of nanotubes”, *Struct. Eng. Mech.*, **57**(1), 179-200.
- Gelin, B.R. (1994), *Molecular Modeling of Polymer Structures and Properties*, Carl Hanser Verlag, Munich, Germany.
- Hajnayeb, A. and Khadem, S.E. (2015), “An analytical study on the nonlinear vibration of a double-walled carbon nanotube”, *Struct. Eng. Mech.*, **54**(5), 987-998.
- Hanchen, H. and Ghoniem, N. (1993), “Neutron displacement damage cross sections for SiC”, *J. Nucl. Mater.*, **199**(3), 221-230.
- Huczko, A., Bystrzejewski, M., Lange, H., Fabianowska, A., Cudzilo, S., Panas, A. and Szala, M. (2005), “Combustion synthesis as a novel method for production of 1-D SiC nanostructures”, *J. Phys. Chem. B*, **109**(34), 16244-16251.
- Khani, N., Fakhraabadi, M.M.S., Vahabi, M. and Kamkari, B. (2014), “Modal analysis of silicon carbide nanotubes using structural mechanics”, *Appl. Phys. A*, **116**(4), 1687-1694.
- Le, M.Q. (2014a), “Young’s modulus prediction of hexagonal nanosheets and nanotubes based on dimensional analysis and atomistic simulations”, *Meccanica*, **49**(7), 1709-1719.
- Le, M.Q. (2014b), “Atomistic study on the tensile properties of hexagonal AlN, BN, GaN, InN and SiC sheets”, *J. Comput. Theor. Nanosci.*, **11**(6), 1458-1464.
- Leach, A.R. (1996), *Molecular Modeling Principles and Applications*, Addison Wesley Longman Limited, London, England.
- Li, C. and Chou, T.W. (2004), “Elastic properties of single-walled carbon nanotubes in transverse directions”, *Phys. Rev. B*, **69**(7), 073401.
- Lin, Z.J., Wang, L., Zhang, J., Guo, X.Y., Yang, W., Mao, H.K. and Zhao, Y. (2010), “Nanoscale twinning-induced elastic strengthening in silicon carbide nanowires”, *Scripta Mater.*, **63**(10), 981-984.
- Morkoc, H., Strite, S., Gao, G.B., Lin, M.E., Sverdlov, B. and Burns, M. (1994), “Large-band-gap SiC, III-V nitride, and II-VI ZnSe-based semiconductor device technologies”, *J. Appl. Phys.*, **76**(3), 1363-1398.
- Nhut, J.M., Vieira, R., Pesant, L., Tessonnier, J.P., Keller, N., Ehret, G., Pham-Huu, C. and Ledoux, M.J. (2002), “Synthesis and catalytic uses of carbon and silicon carbide nanostructures”, *Catal. Today*, **76**(1), 11-32.
- Odegard, G.M., Gates, T.S., Nicholson, L.M. and Wise, K.E. (2002), “Equivalent-continuum modeling of nano-structured materials”, *Compos. Sci. Technol.*, **62**(14), 1869-1880.
- Pan, H. and Si, X. (2009), “Molecular dynamics simulations of diameter dependence tensile behavior of silicon carbide nanotubes”, *Physica B: Condens. Mat.*, **404**(12), 1809-1812.
- Pei, L.Z., Tang, Y.H., Chen, Y.W., Guo, C., Li, X.X., Yuan, Y. and Zhang, Y. (2006), “Preparation of silicon carbide nanotubes by hydrothermal method”, *J. Appl. Phys.*, **99**(11), 114306.
- Persson, C. and Lindefelt, U. (1996), “Detailed band structure for 3C-, 2H-, 4H-, 6H-SiC, and Si around the fundamental band gap”, *Phys. Rev. B*, **54**(15), 10257.
- Rouhi, S. and Ansari, R. (2012), “Atomistic finite element model for axial buckling and vibration analysis of single-layered graphene sheets”, *Physica E: Low-Dimens. Syst. Nanostruct.*, **44**(4), 764-772.
- Rouhi, S., Ansari, R. and Shahnazari, A. (2016), “Vibrational characteristics of single-layered boron nitride nanosheet/single-walled boron nitride nanotube junctions using finite element modeling”, *Mater. Res. Express*, **3**(12), 125027.
- Setoodeh, A.R., Jahanshahi, M. and Attariani, H. (2009), “Atomistic simulations of the buckling behavior of perfect and defective silicon carbide nanotubes”, *Comput. Mater. Sci.*, **47**(2), 388-397.
- Shahnazari, A., Ansari, R. and Rouhi, S. (2017), “A density functional theory-based finite element method to study the vibrational characteristics of zigzag phosphorene nanotubes”, *Appl. Phys. A*, **123**(4), 263.
- Sun, X.H., Li, C.P., Wong, W.K., Wong, N.B., Lee, C.S., Lee, S.T. and Teo, B.K. (2002), “Formation of silicon carbide nanotubes and nanowires via reaction of silicon (from disproportionation of silicon monoxide) with carbon nanotubes”, *J. Am. Chem. Soc.*, **124**(48), 14464-14471.
- Wang, Z.G., Li, J.B., Gao, F. and Weber, W.J. (2010), “Tensile and compressive mechanical behavior of twinned silicon carbide nanowires”, *Acta Mater.*, **58**(6), 1963-1971.
- Zhang, A., Gu, X., Liu, F., Xie, Y., Ye, X. and Shi, W. (2012), “A study of the size-dependent elastic properties of silicon carbide nanotubes: First-principles calculations”, *Phys. Lett. A*, **376**(19), 1631-1635.

CC